JOURNAL OF SOLID STATE CHEMISTRY 116, 422–426 (1995)

Crystal Structure of Ammonium Trimolybdate Monohydrate $(NH_4)_2Mo_3O_{10} \cdot H_2O$ by Powder Diffraction Method

W. Lasocha

Faculty of Chemistry, Jagiellonian University, Ingardena 3, 30-060 Krakow, Poland

and

J. Jansen and H. Schenk

Laboratory for Crystallography, University of Amsterdam, Nieuwe Achtergracht 166, 1018 WV Amsterdam, The Netherlands

Received December 29, 1993; in revised form July 29, 1994; accepted September 29, 1994

The structure of the fibrillar ammonium trimolybdate monohydrate $(NH_4)_2Mo_3O_{10} \cdot H_2O$ was solved by the Direct Method and Powder Diffraction package POWSIM, and refined by the Rietveld method to $R_F = 6.4$ and $R_{wp} = 17.1\%$. Distorted edge-shared MoO_6 octahedra (Mo–O = 1.71–2.62) form infinite chains, built up of Mo_3O_{10} units, parallel to the [010] axis. The space group is $P2_1/m$ (11), with lattice parameters $a = 9.638(1)$, $b = 7.577(2)$, $c = 8.537(1)$ Å, $\beta = 112.89(1)°$, $V = 574.4(2)$ Å^3, $Z = 2$. © 1995 Academic Press, Inc.

INTRODUCTION

Most trimolybdates obtained by precipitation from solutions form fibrillar crystals not suitable for single crystal analysis. Sometimes, if crystals grow into bundles of numerous fibers, Weissenberg photographs of zero and next layers can be obtained (1–3). Using a bunch of parallel oriented fibers of ammonium trimolybdate monohydrate $(NH_4)_2Mo_3O_{10} \cdot H_2O$, a projection of the Patterson function on a plane perpendicular to the fiber axis was calculated (3), and approximate positions of the heavy atoms and of a few oxygen atoms were deduced from it. Recently, the structure of a high pressure form of anhydrous ammonium trimolybdate obtained by high-pressure–high-temperature decomposition of ammonium heptamolybdate was solved (4). The space group, density, and calculated diffraction pattern of this salt differ from the same data from trimolybdate monohydrate (3), even though the Mo–O chains appear to be very similar. However, a full comparison of the two structures is not possible, since the structure of the monohydrate is only partially known. A new form of $(NH_4)_2Mo_3O_{10} \cdot xH_2O$ was detected recently by us in fresh, wet precipitate of ammonium trimolybdate (5). The diffraction pattern of this compound changes very quickly with loss of water. All observations encouraged us to undertake the redetermination of the $(NH_4)_2Mo_3O_{10} \cdot H_2O$ crystal structure, using modern powder diffraction procedures.

EXPERIMENTAL

Fibrillar ammonium trimolybdate monohydrate was obtained by slow crystallization from acidified solution of ammonium heptamolybdate according to a published procedure (3). Sample was pressed into holder according to the so-called "back-packed technique" to minimize texture. Intensity data were collected with a Philips APD 3720 diffractometer system equipped with a sample spinner, compensating slit and diffracted beam graphite monochromator. Data collection details are given in Table 1. The measured intensity data were multiplied by the factor $1/\sin\theta$ to correct for the θ compensating slit (6).

STRUCTURE SOLUTION AND REFINEMENT

The pattern decomposition was done by the program LSQPROF (7). For the structure determination θ range from 8 to 70° was used. The R factor of pattern decomposition was 2.24%. Assuming 0.5 FWHM (full-width at half maximum) as a separation limit, the single reflections file contained 85 intensities while in the overlapping reflections file there were 198 lines. In each cycle of the successive intensity estimation procedure DOREES (8), 5 strong and 10 weak reflections were added to the single reflection file. In cycles 1 and 2 the Patterson map criterion was not applied. After four cycles of the intensity estimating procedure the file of single intensities contained 167 reflections, 61 with E values greater than 1. At this stage the structure solution program SIMPEL88 (9) was run. Only reflections with $|E| \geq 1$ were used for the triplets calculations by TRIQUA (9). On the resulting E-

0022-4596/95 $6.00

TABLE 1
Details of Data Collection and Structure Refinement

Diffractometer	PW 3720
Wavelength	CuK_α
2θ range	8–86
Step scan increment	0.025
Count time [sec/step]	14
Standard peak: $hk1$, 2θ	100, 9.94
R for standard peak [%]	2.8
Space group	$P2_1/m$ (11)
a [Å]	9.638 (1)
b [Å]	7.577 (2)
c [Å]	8.537 (1)
β [°]	112.89 (1)
V [Å^3]	574.4 (2)
Number of observations	3024
Number of structural parameters refined	37
Number of reflections	450
Number of profile parameters	10
R_F	6.4
R_I	10.6
R_{wp}	17.1
R_{exp}	8.1
Preferred orientation, vector and factor	[010], −0.23(2)
Max. shift/error	0.02

map 2 molybdenum atoms and 5 oxygen atoms were easily located. The structure solution procedure was continued by the Rietveld method using a PC version of the XRS-82 program (10). Because the Rietveld refinement was unstable the soft constraints on some Mo–O and O–O bond lengths had to be introduced. After a few cycles of constrained refinement missing atoms were sought on difference Fourier maps. This procedure was repeated until all nonhydrogen atoms were found. Discrepancy factors were high: $R_F = 15.8$, $R_I = 25.4$, $R_{wp} = 18.0\%$. Relevant plots can be found in Fig. 1A.

It was surprising that although the structure is solved easily, it is difficult to refine by the Rietveld method. This could be caused by the appearance of two very strong peaks at 9.94° and 11.21°, whereas at higher angles there are only weak and very weak peaks (see Fig. 1A). As a result the minimizing quantity in the Rietveld refinement is dominated by two peaks, and thus constraints are necessary. In addition we assume that the presence of the LP factor in the quantity minimized by the least-squares procedure is unfavorable for high angular range of diffraction pattern. The LP factor can obscure even large differences between F_o and F_c, because for high angles (e.g., $2\theta \geq 60$) the observed intensities are usually very small and the difference pattern (important for the least-squares algorithm) is accordingly flattered. In order to check this hypothesis in a second approach with Rietveld refinement a pattern corrected for the LP factor was used, in which the pattern was no longer dominated by any peak. Now the structure could be refined without any geometrical constraints. The R factors are $R_F = 6.4$, $R_I = 10.6$, $R_{wp} = 17.1\%$. The observed, calculated, and difference plots for refinement of the data (corrected by the LP factor) are presented in Fig. 1B. Since the LP-corrected diffraction pattern is more noisy than the original pattern, R_{wp} is slightly lower than in the case of the previous refinement, but R_F and R_I are much better.

The largest differences between the observed and calculated patterns occur for the 040 reflection. However, its intensity and the value of its structure factor are reproduced with errors of 3.9 and 1.7%, respectively. The source of error is that the 040 line is narrower than the other lines, as [010] is the needle axis and the direction of preferred orientation. Refinement of individual temperature factors for oxygen atoms did not improve the R factors and caused the refinement to be unstable. Thus, two temperature factors for oxygen in the Mo–O chains were refined, one for shared and one for unshared oxygen atoms. The positions of the NH_4^+ ions and the water molecule were not distinguished by the X-ray methods; their positions were assigned so that the ammonium was surrounded by oxygen atoms only. Disorder or partial occupancy of positions occupied by water molecules, observed in similar compounds (11, 12), is possible, as suggested by the high value of its temperature factor.

STRUCTURE DESCRIPTION AND DISCUSSION

Final atomic coordinates and selected interatomic distances are listed in Table 2. Figure 2A presents the projection of the structure on the (010) plane. The structure consist of distorted MoO_6 octahedra which are edge-shared to form $Mo_3O_{10}^{2-}$ units, linked together to form infinite chains parallel to [010]. The $Mo_3O_{10}^{2-}$ chains in polyhedral representation are presented in Fig. 3A. Each molybdenum atom has two terminal oxygen atoms in *cis* position to one another. The Mo(1)–O and Mo(2)–O distances range from 1.71 to 2.62 and from 1.78 to 2.51 Å. Distortions of MoO_6 octahedra, reflected by the bond-length dispersion, are rather prominent, but are only partially caused by the low precision of powder experiments. As in most structures built up of linked MoO_6 octahedra, distortions are caused by mutual repulsion of metal atoms. In a group of two octahedra linked by a common edge the Mo atoms diverge towards the terminal atoms, that is, from one another, by 0.3–0.6 Å (13). Between parallel chains there are water molecules and NH_4^+ cations.

The same type of Mo_3O_{10} chains are present in the hydrated forms of rubidium, silver, and potassium trimolybdate and in the high pressure form of the ammonium analogue (4, 12, 14, 15). By X-ray diffraction methods it was found that the structures of all known trimolybdates are composed of infinite chains of polymolybdate anions.

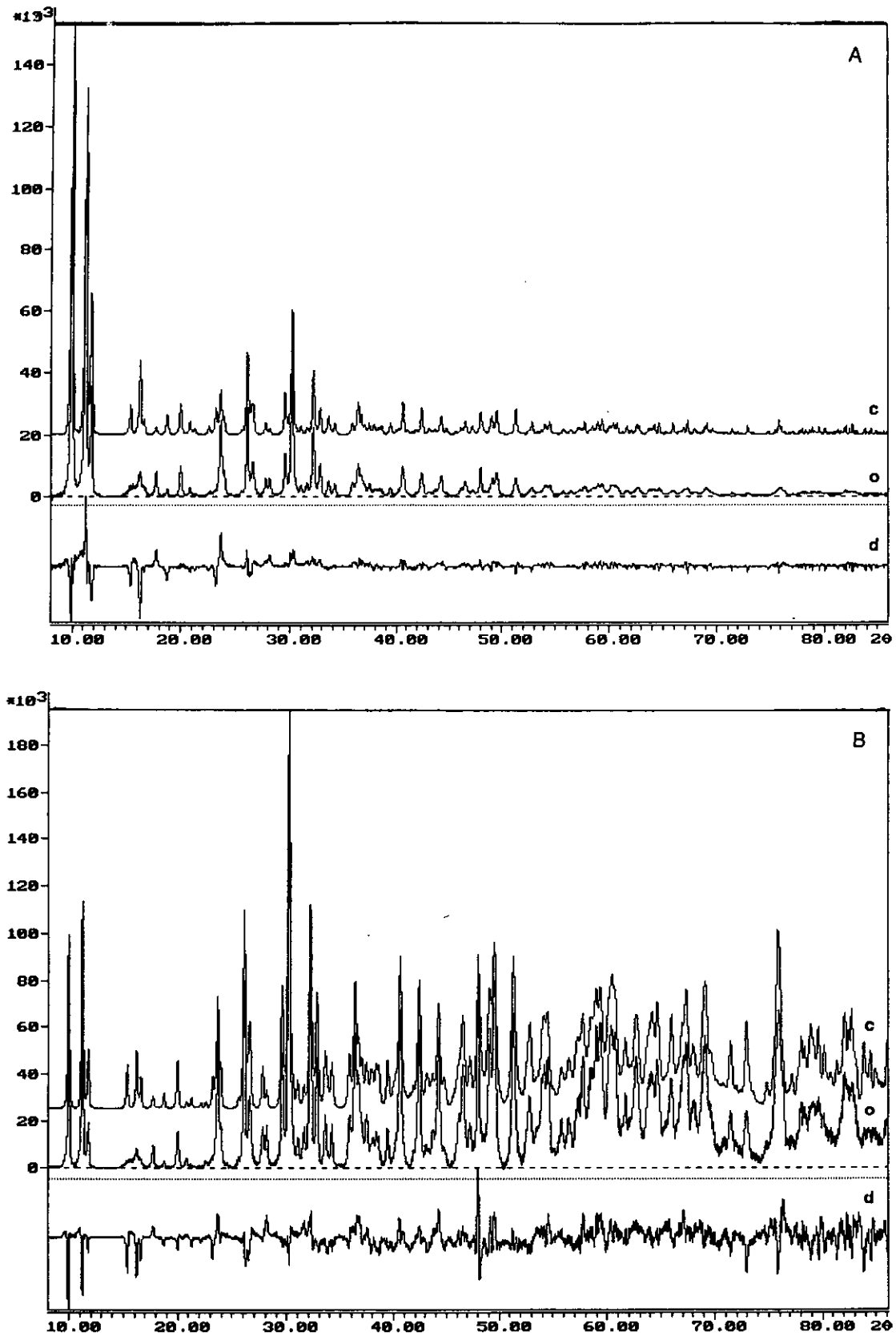

FIG. 1. Observed (o), calculated (c), and difference (d) pattern for $(NH_4)_2Mo_3O_{10} \cdot H_2O$ not corrected by LP factor (A), and after correction (B).

TABLE 2
List of Atomic Parameters and Selected Interatomic Distances

Atom	x	y	z	U
Mo(1)	0.134 (2)	0.2500	0.245 (2)	0.029(4)
Mo(2)	0.1667(9)	−0.001 (2)	−0.048(1)	0.022(2)
O(1)	0.886 (6)	0.030 (8)	0.820(6)	0.01 (1)
O(2)	0.342 (9)	0.2500	0.36 (1)	0.012(9)
O(3)	0.10 (1)	0.2500	0.43 (1)	0.012
O(4)	0.148 (5)	0.02 (1)	0.725(6)	0.012
O(5)	0.19 (1)	0.2500	0.01 (1)	0.01
O(6)	0.362 (6)	−0.026 (9)	1.080(6)	0.012
O(7)	0.85 (1)	0.2500	0.03 (1)	0.01
O(8)[a]	0.62 (3)	0.2500	0.30 (3)	0.11 (9)
N(1)	0.91 (1)	0.2500	0.59 (2)	0.01 (3)
N(2)	0.41 (1)	0.2500	0.71 (1)	0.00 (3)

Mo(1)–O(3)	1.73 (12)	Mo(2)–O(6)	1.78 (5)
O(2)	1.86 (8)	O(4)	1.88 (5)
O(1)	2.18 (6)	O(7)	1.90 (3)
O(1)	2.18 (6)	O(5)	1.96 (3)
O(5)	2.27 (11)	O(1)	2.21 (6)
O(7)	2.62 (8)	O(1)	2.50 (5)
Mo(1)–Mo(2)	3.25 (2)	Mo(2)–Mo(2)	3.61 (1)
Mo(2)	3.32 (2)		

[a] Water molecule.

Figure 3 presents the three types of polymolybdate anions detected so far, in polyhedral representation. Ammonium molybdate and similar compounds mentioned above are shown in Fig. 3A. Only slightly different, chains straight instead of zigzag, is the anion of $[(CH_3)_2NH_2]_4Mo_6O_{20} \cdot 2H_2O$ (2) presented in Fig. 3B. This compound described by authors as hexamolybdate by stoichiometry belongs to the trimolybdates. The third type of trimolybdate anion was detected in $K_2Mo_3O_{10}$,

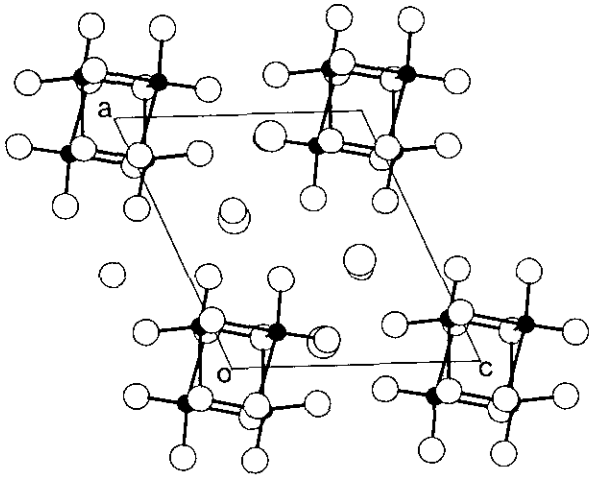

FIG. 2. Projection of the structure of $(NH_4)_2Mo_3O_{10} \cdot H_2O$ along the *b* axis. The small black circles represent molybdenum atoms. Large and medium circles are nitrogen and oxygen atoms, respectively.

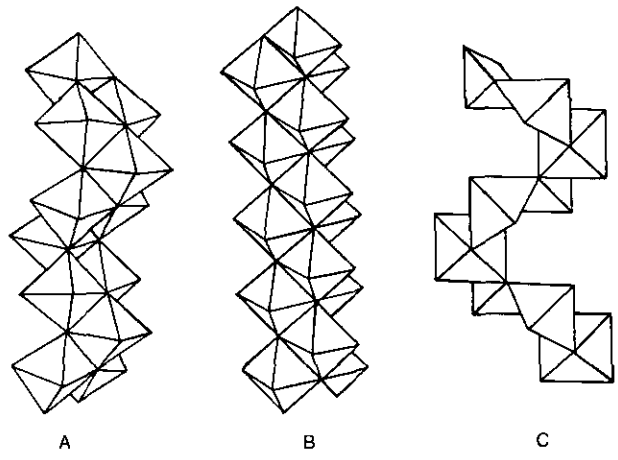

FIG. 3. Polyhedral representation of anions: (A) $(NH_4)_2Mo_3O_{10} \cdot H_2O$ and compounds described in (4, 12, 14, 15): (B) $[(CH_3)_2NH_2]_4Mo_6O_{20} \cdot 2H_2O$ (2): (C) $K_2Mo_3O_{10}$ (16).

obtained by fusion of K_2CO_3 and MoO_3 (16). Its structure contains distorted MoO_6 octahedra and MoO_5 square pyramids which share edges to form infinite chains, Fig. 3C.

Though they have the same type of anion, the crystal structures of monoclinic $(NH_4)_2Mo_3O_{10} \cdot H_2O$ and the high pressure form $(NH_4)_2Mo_3O_{10}$ are different. In the high pressure form, infinite chains form a rectangular network, having the same chain in the centers of the rectangles twisted about 90° and translated by $\frac{1}{2}b$, to assure the best fit to neighboring zigzag chains. The space group of the high pressure form is *Pnma* (62), which is the minimal nonisomorphic supergroup of $P2_1/m$. However, compounds have different compositions and have been synthesized following different methods. So even though relations between lattices can be found (e.g., the same *b* period), the problem of their mutual transformations was not investigated in detail.

ACKNOWLEDGMENT

Support of the Polish Committee of Science Research (KBN, 0096/P3/93/05) and of the Foundation of Crystallographic Studies through a Carolina H. MacGillary stipend is kindly acknowledged.

REFERENCES

1. J. Chojnacki and S. Hodorowicz, *Rocz. Chem.* **47,** 2213 (1973).
2. H. Toraya, F. Marumo, and T. Yamase, *Acta Crystallogr. Sect. B* **40,** 145 (1984).
3. S. A. Hodorowicz and W. Lasocha, *Cryst. Res. Technol.* **23** (2), K43 (1988).
4. K-J. Range, A. Foessler, *Acta Crystallogr. Sect. C* **46,** 488 (1990).
5. W. Lasocha, to be published.
6. D. L. Bish and J. E. Post (Eds.), "Modern Powder Diffraction," *Rev. Mineral.* **20** (1989).
7. J. Jansen, R. Peschar, and H. Schenk, *J. Appl. Crystallogr.* **25,** 231 (1992).

8. J. Jansen, R. Peschar, and H. Schenk, *J. Appl. Crystallogr.* **25,** 237 (1992).
9. J. Jansen, R. Peschar, and H. Schenk, *Z. Krist.* **206,** 33 (1993).
10. Ch. Baerlocher, "XRS-82, X-Ray Rietveld system." Institut für Kristalographie, Eidgenössische Technische Hochschule, Zurich, 1982. (PC version of XRS-82: D. Mucha and W. Lasocha., *J. Appl. Crystallogr.* **27,** 201 (1994).)
11. B. Krebs and I. Paulat-Boshen, *Acta Crystallogr. Sect. B* **32,** 1697 (1976).
12. H-U. Kreusler, A. Foerster, and J. Fuchs, *Z. Naturforsch. B* **35,** 242 (1980).
13. M. A. Porai-Koshits and L. O. Atovmyan, *Russ. J. Inorg. Chem.* **26,** 1697 (1981).
14. W. Lasocha, J. Jansen, and H. Schenk, *J. Solid State Chem.* **109,** 1 (1994).
15. W. Lasocha, J. Jansen, and H. Schenk, *J. Solid State Chem.*, in press.
16. B. M. Gatehouse and P. Leverett, *J. Chem. Soc.* **A,** 1398 (1968).